HHS Public Access

Author manuscript

Cell. Author manuscript; available in PMC 2016 February 12.

Published in final edited form as:

Cell. 2015 February 12; 160(4): 595–606. doi:10.1016/j.cell.2015.01.009.

A Micropeptide Encoded by a Putative Long Non-coding RNA Regulates Muscle Performance

Douglas M. Anderson[1], **Kelly M. Anderson**[1], **Chi-Lun Chang**[2], **Catherine A. Makarewich**[1], **Benjamin R. Nelson**[1], **John R. McAnally**[1], **Prasad Kasaragod**[1], **John M. Shelton**[3], **Jen Liou**[2], **Rhonda Bassel-Duby**[1,4], and **Eric N. Olson**[1,4,*]

[1]Department of Molecular Biology, The University of Texas Southwestern Medical Center, 5323 Harry Hines Boulevard, Dallas, TX 75390–9148, USA

[2]Department of Physiology, The University of Texas Southwestern Medical Center, 5323 Harry Hines Boulevard, Dallas, TX 75390–9148, USA

[3]Department of Internal Medicine, The University of Texas Southwestern Medical Center, 5323 Harry Hines Boulevard, Dallas, TX 75390–9148, USA

[4]Hamon Center for Regenerative Science and Medicine, The University of Texas Southwestern Medical Center, 5323 Harry Hines Boulevard, Dallas, TX 75390–9148, USA

Summary

Functional micropeptides can be concealed within RNAs that appear to be non-coding. We discovered a conserved micropeptide, that we named myoregulin (MLN), encoded by a skeletal muscle-specific RNA annotated as a putative long non-coding RNA. MLN shares structural and functional similarity with phospholamban (PLN) and sarcolipin (SLN), which inhibit SERCA, the membrane pump that controls muscle relaxation by regulating Ca^{2+} uptake into the sarcoplasmic reticulum (SR). MLN interacts directly with SERCA and impedes Ca^{2+} uptake into the SR. In contrast to PLN and SLN, which are expressed in cardiac and slow skeletal muscle in mice, MLN is robustly expressed in all skeletal muscle. Genetic deletion of MLN in mice enhances Ca^{2+} handling in skeletal muscle and improves exercise performance. These findings identify MLN as an important regulator of skeletal muscle physiology and highlight the possibility that additional micropeptides are encoded in the many RNAs currently annotated as non-coding.

Introduction

Ca^{2+} controls the normal function of striated muscle by acting as the primary regulator of the sarcomeric contractile machinery and as a second messenger in the signal transduction pathways that control muscle growth, metabolism and pathological remodeling (Bassel-

*Correspondence to:eric.olson@utsouthwestern.edu.

Duby and Olson, 2006; Berchtold et al., 2000). Ca^{2+} handling in striated muscle is tightly regulated by Ca^{2+} pumps in the sarcoplasmic reticulum (SR) and plasma membranes that maintain intracellular Ca^{2+} levels ~10,000-fold lower than extracellular and SR concentrations (Berridge et al., 2003; Rossi and Dirksen, 2006). Upon muscle stimulation, Ca^{2+} release by the ryanodine receptor (RyR) in the SR membrane transiently increases Ca^{2+} levels in the cytosol, triggering actomyosin cross-bridge formation within the sarcomere to generate contractile force. Reuptake of Ca^{2+} into the SR by sarcoplasmic reticulum Ca^{2+}-ATPase (SERCA) is necessary for muscle relaxation and restores SR Ca^{2+} levels for subsequent contraction-relaxation cycles. SERCA serves as a central regulator of striated muscle performance and the pathological signaling pathways that drive cardiovascular and skeletal muscle disease (Dorn and Molkentin, 2004; Goonasekera et al., 2011; Odermatt et al., 1996; Pan et al., 2003; Periasamy and Kalyanasundaram, 2007).

Two related peptides, phospholamban (PLN) and sarcolipin (SLN) directly interact with SERCA in the SR membrane to regulate Ca^{2+} pump activity (Kranias and Hajjar, 2012; MacLennan and Kranias, 2003; Schmitt et al., 2003). PLN and SLN are expressed in partially overlapping patterns in cardiac and slow skeletal muscle and are important regulators of muscle performance and cardiovascular disease (Briggs et al., 1992; Kranias and Hajjar, 2012; Minamisawa et al., 2003; Tada and Toyofuku, 1998; Tupling et al., 2011). PLN-deficient mice exhibit enhanced myocardial contractile performance, characterized by increased ventricular relaxation rates and SERCA pump activity (Chu et al., 1998; Luo et al., 1994). Similarly, loss of PLN or SLN expression significantly increases the rate of muscle relaxation and SERCA pump activity in slow skeletal muscle, but does not affect fast skeletal muscles, which do not express PLN or SLN (Slack et al., 1997; Tupling et al., 2011; Vangheluwe et al., 2005). The absence of PLN and SLN expression in fast skeletal muscle, the dominant muscle type in mice, suggests that an unidentified factor regulates Ca^{2+} handling and the contractile performance of this tissue.

Recent genome-wide studies have suggested that hundreds of functional micropeptides may be encoded in vertebrate long non-coding RNAs (lncRNAs) (Andrews and Rothnagel, 2014; Bazzini et al., 2014). The microproteome has largely been overlooked in gene annotations, primarily due to the difficulty in identifying functional small open reading frames (ORFs) in RNA transcripts. While analyzing an annotated skeletal muscle-specific lncRNA, we discovered a previously unrecognized ORF encoding a conserved 46 amino acid micropeptide, that we named myoregulin (MLN). MLN forms a single transmembrane alpha helix that interacts with SERCA in the membrane of the SR and regulates Ca^{2+} handling. Consistent with this function, deletion of MLN in mice significantly enhances Ca^{2+} handling and improves exercise performance. These findings identify MLN as the predominant SERCA-inhibitory micropeptide in skeletal muscle, which surprisingly was concealed in an RNA annotated as non-coding.

Results

Discovery of a Conserved Micropeptide Encoded By a LncRNA

In a bioinformatic screen for uncharacterized skeletal muscle-specific genes, we identified a vertebrate RNA transcript annotated as a lncRNA (LINC00948 in humans and AK009351 in

mice). Analysis of the evolutionary conservation of these transcripts identified a short 138 nucleotide ORF with the potential to encode a highly conserved 46 amino acid micropeptide, which we named myoregulin (MLN) (Figure S1A). The human and mouse MLN genes consist of three exons that span 16.5 and 15.0 kilobases (kb), respectively, with the ORF located in exon 3 (Figure 1A). Nucleotide insertions and deletions that could alter the reading frame flank the MLN ORF, demonstrating that these sequences comprise untranslated regions (UTRs) (Figure S1A).

During embryogenesis, MLN is expressed in the myotomal compartment of the somites, the anlagen of skeletal muscle (Figure 1B). During fetal and adult stages, MLN is robustly expressed in all skeletal muscles and is not detectable in cardiac or smooth muscles (Figure 1B and 1C). MLN transcripts are also present in C2C12 myoblasts and myotubes, but not in 10T1/2 fibroblasts (Figure S1B).

To determine if the MLN ORF is translated as a micropeptide, we transcribed and translated the full-length MLN RNA in vitro in the presence of radiolabeled ^{35}S-methionine (Figure 1D and 1E). A single ∼5 kDa micropeptide was produced from the MLN transcript, whereas a frameshift mutation that disrupted the MLN ORF abolished any detectable expression (Figure 1D and 1E). We further cloned a FLAG epitope tag in-frame with the C-terminus of the MLN coding sequence within the full-length MLN transcript (Figure S1C). Expression of this construct in COS7 cells yielded a peptide of ∼6 kDa, corresponding to the predicted molecular weight of the MLN-FLAG fusion peptide, detected by western blot (Figure S1D).

To determine whether MLN is endogenously expressed in skeletal muscle, we introduced the same FLAG epitope tag into the MLN locus in C2C12 muscle cells using CRISPR/Cas9-mediated homologous recombination (Figure 1F and S1E). PCR-based genotyping and restriction fragment length polymorphism (RFLP) analyses were used to verify correct targeting (Figure 1G and S1F). As shown by western blot analysis in Figure 1H, C2C12 cells heterozygous for the MLN-FLAG knock-in allele expressed a micropeptide of the predicted molecular weight of the MLN-FLAG fusion peptide. Together, these data reveal that the MLN RNA, which is annotated as non-coding, in fact encodes a cryptic micropeptide.

MLN Encodes a Transmembrane Alpha Helix

The MLN micropeptide is highly conserved across mammals and is predicted to form a type II single-pass transmembrane alpha helix, in which the 19 N-terminal amino acid residues are exposed to the cytosol and the 3 C-terminal residues are lumenal (Figure 2A and S2A). The N-terminal residues (5–10) of MLN are predicted to fold into a small beta sheet and the C-terminal half of the protein contains the predicted transmembrane alpha helix (Figure 2A and S2A). Circular dichroism spectroscopy measurements of synthesized full-length MLN peptide in detergent micelles confirmed it consists of alpha helix (43.6%), beta sheet (21.1%), turn (9.6%) and random coil (25.7%) structures (Figure S2B).

Association of MLN with SERCA

MLN shows a strong structural resemblance to PLN and SLN, which also form type II single-pass transmembrane peptides oriented with their N-terminal residues exposed to the

cytosol. Sequence alignment of MLN, PLN and SLN revealed a number of identically conserved residues in their transmembrane regions, which are also found in the invertebrate ortholog, sarcolamban (SCL) (Figure 2A) (Magny et al., 2013). Structural modeling of the transmembrane helices showed that all four peptides are predicted to form alpha helical structures with residues arranged in a similar spatial pattern (Figure 2B). PLN and SLN both interact with SERCA in the membrane of the SR in a common groove formed by the M2, M6 and M9 helices of SERCA (Figure 2C) (Toyoshima et al., 2003; Toyoshima et al., 2013; Winther et al., 2013). Automated protein docking of the transmembrane model of MLN with the crystal structure of SERCA revealed that MLN aligned in the same groove that is occupied by PLN and SLN (Figure 2C).

MLN is Embedded in the SR Membrane and Co-localizes with SERCA1

To examine the subcellular localization of MLN in vivo, we electroporated a plasmid encoding green fluorescent protein fused to MLN (GFP-MLN) into the flexor digitorum brevis muscle of adult mice. Two-photon laser scanning confocal microscopy allowed for the simultaneous detection of GFP fluorescence and second harmonic generation (SHG) to visualize the myosin A band of the sarcomeres (Nelson et al., 2013). The GFP-MLN fusion protein localized in a repeating pattern that alternated with the myosin A band and overlapped with the localization of an mCherry-SERCA1 fusion protein within the SR (Figure 2D). This pattern was consistent with the localization of GFP-PLN and GFP-SLN fusion proteins (Figure S2C). Additionally, an N-terminal HA-tagged MLN fusion protein (HA-MLN) expressed in C2C12 myoblasts was enriched in the subcellular fraction containing SR/ER membrane proteins (Figure 2E), altogether suggesting that MLN functions in the membrane of the SR.

In co-immunoprecipitation experiments, the HA-MLN fusion protein formed a stable complex with SERCA1 (skeletal muscle-specific), SERCA2a (cardiac and slow skeletal muscle-specific) and SERCA2b (ubiquitous) isoforms (Figure S2D). Alanine mutagenesis of MLN residues shared with PLN and SLN (L29A, F30A, and F33A) abolished the ability of MLN to interact with SERCA1, whereas mutation of charged residues (K27A, D35A) did not alter this interaction (Figure 2F). These findings suggest that MLN, PLN and SLN share a common hydrophobic binding motif that stabilizes their association with SERCA.

MLN Regulates Ca^{2+} Handling by Inhibiting SERCA Pump Activity

PLN and SLN both function to inhibit Ca^{2+} re-uptake into the SR by lowering the affinity of SERCA for Ca^{2+}, without altering the maximal rate of Ca^{2+} pump activity (Vmax). To determine if MLN regulates SERCA activity in a similar manner, we directly measured Ca^{2+}-dependent Ca^{2+}-ATPase activity in homogenates from HEK 293 cells expressing SERCA1 (Figure 3A). Similar to the effects of PLN and SLN, expression of MLN caused a significant reduction in the rate of Ca^{2+} uptake, measured as an increase in K_{Ca} (Figure 3A and Table S1). Co-expression of the full-length RNA encoding MLN (MLN RNA) resulted in a similar decrease in Ca^{2+} uptake compared to a vector containing only the MLN coding sequence (Figure 3B). The activity of the MLN RNA was abolished by introduction of a frameshift mutation to disrupt the expression of the MLN micropeptide (MLN-RNA-FS), demonstrating that the RNA itself does not inhibit SERCA activity (Figure 3B). No effects

on *V*max were observed under any conditions tested and the addition of thapsigargin, a potent inhibitor of SERCA activity, abolished Ca^{2+} uptake (Figure 3A).

Since the concentration of SR Ca^{2+} is dependent upon SERCA re-uptake activity, we examined if MLN over-expression could alter SR Ca^{2+} levels in C2C12 myoblasts. SR Ca^{2+} levels were directly measured using retroviral delivery of the FRET–based, SR-localized Ca^{2+} sensor T1ER, using culture conditions previously shown to be sensitive to changes in endogenous SERCA activity (Brandman et al., 2007). Co-expression of MLN or SLN significantly decreased the levels of SR Ca^{2+}, measured as a decrease in T1ER FRET (Figure 3C). We alternatively compared SR Ca^{2+} levels using the ratiometric Ca^{2+} indicator dye fura-2-AM, following SR Ca^{2+} release using the RyR agonist 4-Chloro-M-Cresol (4-CMC) (Figure 3D). Consistent with our previous findings, over-expression of MLN or SLN significantly decreased peak Ca^{2+} release from the SR (Figure 3D). Together, these findings demonstrate that MLN inhibits SERCA pump kinetics similar to PLN and SLN.

MLN, PLN and SLN are Expressed in Different Striated Muscle Types

The structural and functional similarities between MLN, PLN and SLN suggest they comprise a family of micropeptides that regulate Ca^{2+} handling through modulation of SERCA activity. To determine if PLN or SLN are functionally redundant with MLN in vivo, we examined their expression during developmental and adult stages. In the heart, PLN expression was detectable in both the atria and ventricles, whereas SLN expression was specific to the atria (Figure 4A and Figure S3A). SLN overlapped with the expression of MLN in fetal skeletal muscles, which display a slow phenotype during embryonic development (Figure S3A) (Lu et al., 1999). Consistent with previous reports, quantitative real-time PCR and RNA-seq expression analyses revealed that SLN was markedly down-regulated in most adult skeletal muscles, which convert to fast type in the mouse (Figure 4A and Figure S3B) (Tupling et al., 2011). In contrast, MLN was robustly expressed in all adult skeletal muscles, similar to the expression pattern of SERCA1 (Figure 4A and 4B). The expression patterns of PLN and SLN were more similar to the expression of SERCA2, which is highly expressed in cardiac and slow skeletal muscles (Figure 4B). In addition, comparison of RNA-seq expression data revealed that PLN and SLN are not expressed in differentiated C2C12 myotubes, whereas MLN transcripts are robustly expressed (Figure S3C). Thus, MLN, PLN and SLN are differentially expressed across vertebrate muscle types and MLN is the most abundant of the three micropeptides expressed in adult skeletal muscle of the mouse.

Transcriptional Control of MLN Expression by MyoD and MEF2

MLN and the skeletal muscle-specific isoforms of SERCA and RyR are co-regulated by MyoD, suggesting they comprise a core genetic module important for Ca^{2+} handling in skeletal muscle (Fong et al., 2012). Analysis of the 5' flanking region of the MLN gene revealed highly conserved binding sites for the myogenic transcription factors MyoD (E-box) and MEF2 (Figure S4A), which bound specifically to these sequences in gel mobility shift assays (Figure S4B). MyoD and MEF2 independently activated a luciferase reporter linked to the proximal MLN promoter (MLN-Luc) and transactivation was lost upon mutagenesis of their respective binding sites (Figure 5A). ChIP-seq data at this locus

revealed that MyoD bound specifically to this region in both C2C12 myoblasts and myotubes (Figure S4C) (Bernstein et al., 2012). The activity of the MLN-Luc promoter in C2C12 myoblasts and myotubes was similarly dependent upon both the MEF2 and E-box sequences which, when mutated, resulted in the loss and abrogation of MLN promoter activation, respectively (Figure 5B). Consistent with this, a LacZ transgene controlled by the MLN promoter (MLN-lacZ) displayed skeletal muscle-specific expression in vivo and was dependent upon the MEF2 and E-box sequences for full promoter activation (Figure 5C). Thus, the MLN gene is a direct target of the core transcription factors that activate skeletal myogenesis.

Generation of MLN Knockout Mice Using TALENs

To investigate the function of MLN in vivo, we generated MLN knockout (KO) mice using TAL effector nuclease (TALEN)-mediated homologous recombination. A unique TALEN pair specific for exon 1 of the MLN locus was designed and constructed using the REAL assembly method (Reyon et al., 2012). A loss of function allele was created using a donor plasmid to insert a red fluorescent reporter (tdTomato) followed by a triple polyadenylation cassette into exon 1 in the MLN locus (Figure 6A). This strategy was designed to prematurely terminate transcription upstream of the MLN coding sequence but allow for the expression of a red fluorescent reporter by the endogenous MLN promoter. Correct targeting was verified by Southern blot and PCR-based genotyping (Figures 6B and Figure S5A). Detection of tdTomato fluorescence in MLN KO mice was specific to skeletal muscle and was not detected in other tissues (Figure 6C). Quantitative PCR using primer pairs specific to the downstream exons 2 and 3 demonstrated that the MLN transcript was absent in skeletal muscle from MLN KO mice (Figure 6D).

MLN KO mice were born at expected Mendelian ratios from heterozygous intercrosses and showed no obvious morphological abnormalities or differences in body or muscle weights (Figure S5B). Mice lacking PLN and SLN also have non-pathological phenotypes but show enhanced Ca^{2+} handling and contractility in cardiac and slow skeletal muscle (Luo et al., 1994; MacLennan and Kranias, 2003; Tupling et al., 2011).

Enhanced Ca^{2+} Handling and Skeletal Muscle Performance in MLN KO Mice

To examine the potential role of MLN in regulating skeletal muscle performance, we subjected 8-week old wild-type (WT) and MLN KO mice to a regimen of forced treadmill running to exhaustion. Remarkably, MLN KO mice ran an average time of ∼31% longer than their WT littermates, representing a 55% increase in running distance (Figure 6E and 6F). Mice with a fast-to-slow fiber type switch also show increased running performance (van Rooij et al., 2009). However, histological analyses of hindlimb muscles, including quadriceps (fast-type) and soleus (slow-type) muscles revealed no obvious differences in fiber-type identity or myofiber size between WT and MLN KO mice (Figure S5C–S5E), indicating that MLN functions through a different mechanism to regulate muscle performance.

We next investigated whether SR Ca^{2+} levels were altered in primary myoblasts isolated from hindlimb muscles of MLN KO versus WT littermates. SR Ca^{2+} levels were measured

using the calcium indicator fura-2-AM and SR Ca^{2+} release by the addition of the RyR agonist 4-CMC. Strikingly, MLN KO myoblasts showed significantly increased SR Ca^{2+} levels compared to WT myoblasts, measured as peak SR Ca^{2+} release (Figure 6G). This increase occurred without changes in the expression of RyR1 and SERCA1 expression between WT and MLN KO muscles (Figure S5F), consistent with the function of MLN as an inhibitor of SERCA activity. Together, these findings support the function of MLN as the dominant regulator of SERCA activity in adult skeletal muscle.

Discussion

SERCA is a key regulator of striated muscle performance by serving as the major Ca^{2+} ATPase responsible for the re-uptake of cytosolic Ca^{2+} into the SR (Figure 7A). Direct modulation of SERCA pump activity by the micropeptides PLN and SLN regulates muscle contractility by diminishing the rate of Ca^{2+} re-uptake into the SR. However, since PLN and SLN are not expressed in most adult skeletal muscles of mice, the possible existence of other SERCA regulatory factors has remained an open question.

Our biochemical and in vivo results show that MLN forms a stable complex with SERCA in the membrane of the SR and that MLN directly influences SR Ca^{2+} levels and maximal exercise performance. The robust skeletal muscle-specific expression of MLN, resulting from direct transactivation by the myogenic transcription factors MyoD and MEF2, further highlight MLN as the predominant SERCA regulating micropeptide in adult skeletal muscle. The discovery of MLN reveals a universal mechanism for the control of SERCA activity by a family of related micropeptides expressed in different striated muscle types in vertebrates (Figure 7A).

Micropeptides can be Concealed within RNAs Misannotated as Non-Coding

Micropeptides remain highly underrepresented in genome annotations due in large part to the difficulty in identifying functional short ORFs in RNA transcripts. Recent advances in bioinformatic and biochemical methodologies have revealed that lncRNAs may harbor concealed micropeptides, however, only a few have been functionally verified and characterized in vivo. Here we have identified and characterized the function of a conserved micropeptide in vertebrates that functions as an important regulator of skeletal muscle performance through modulation of Ca^{2+} handling by SERCA. Given the attention that has been focused on the control of SERCA activity and muscle function over the years, it is remarkable that such a key regulator of these processes has gone undetected. Undoubtedly, this is because the MLN ORF is concealed in an RNA annotated as non-coding. Our discovery of MLN was possible due to its high sequence conservation in vertebrates and the presence of an identifiable functional domain, a type II transmembrane alpha helix. We found that the MLN alpha helix shares residues in common with PLN and SLN, however, common bioinformatic search tools alone are not sufficient to identify the relatedness of MLN, PLN and SLN. Interestingly, both PLN and SLN were first discovered as micropeptides and subsequently mapped to RNA transcripts (Kirchberber et al., 1975; Wawrzynow et al., 1992). The PLN and SLN genes share a genomic architecture similar to that of MLN, in which the small ORFs are encoded in the 5’ region of the terminal exon.

Indeed, the transcripts encoding PLN and SLN may have also been annotated as non-coding, if not for their prior discovery as micropeptides.

A Family of SERCA-inhibitory Micropeptides

In Drosophila, the invertebrate ortholog of SERCA is encoded by a single gene (Ca-P60A) and is modulated by the recently identified micropeptide sarcolamban (SCL) (Magny et al., 2013). In vertebrates, the SERCA family has expanded to encode three genes (SERCA1–3) that give rise to multiple alternate splice variants with differing kinetic properties and expression patterns (Anger et al., 1994; Periasamy and Kalyanasundaram, 2007). The expansion of vertebrate gene families occurred through whole genome and gene duplication events, resulting in the formation of paralogous gene families. Combined with the tissue-specific expression patterns of the individual SERCA isoforms, the differential expression of MLN, PLN and SLN likely contribute to the unique Ca^{2+} handling and contractile properties of different striated muscle types in vertebrates. In addition, the extent to which MLN, PLN and SLN partially overlap in their expression in different muscle types may influence the calcium kinetics and performance of these tissues. Co-expression of PLN and SLN in atrial cardiomyocytes and slow skeletal muscle has been shown to result in the super-inhibition of SERCA pump activity (MacLennan et al., 2003). MLN expression overlaps with that of PLN and SLN in adult slow skeletal muscle and with SLN in developing skeletal muscles. Future biochemical and animal studies are required to determine the extent to which MLN synergizes with PLN and SLN in co-regulating SERCA activity in slow type and developing skeletal muscle. SLN expression in larger animals is more widespread than in rodents, occurring in both fast and slow type muscles (Fajardo et al., 2013; Odermatt et al., 1997). A synergistic interaction between MLN and SLN may be more biologically relevant in the adult tissues of these species, however, the relative expression patterns of these two genes in these species remains to be determined.

Apart from spatio-temporal differences in expression, the SERCA-regulatory peptides differ in size and presence of additional secondary structures. A schematic illustration of the family of SERCA-inhibitory micropeptides is shown in Figure 7B. Both SLN and SCL lack extended N-terminal regions and additional secondary structures other than their transmembrane alpha helices. MLN and PLN have expanded N-terminal cytoplasmic regions that encode a beta-sheet and alpha helix, respectively. The N-terminal sequence of PLN has been shown to be critical for its function, and phosphorylation of Serine-16 by Protein Kinase A (PKA) or Threonine-17 by Ca^{2+}/calmodulin-dependent protein kinase II (CaMKII) diminishes the ability of PLN to inhibit SERCA activity (Mattiazzi et al., 2006; Wegener et al., 1989). The N-terminal sequence of MLN could serve as a similar regulatory domain through phosphorylation, as this sequence contains multiple serine and threonine residues. Deciphering the physiological signaling pathways that regulate MLN expression and function will be important to fully understand its role in skeletal muscle development and disease.

Future Questions

Defects in Ca^{2+} signaling underlie the pathogenesis of many muscle diseases that arise from mutations in components of Ca^{2+} signaling pathways, as well as diseases that arise from a

loss of myofiber structural integrity (Berchtold et al., 2000; Millay et al., 2008). Given the importance of SERCA pump activity in regulating Ca^{2+} handling and the pathogenesis of skeletal muscle diseases, such as Brody myopathy and muscular dystrophies (Allen et al., 2010; Goonasekera et al., 2011; Odermatt et al., 1996), the discovery of MLN opens interesting possibilities for the modulation of these pathways. Considering the enhanced exercise capacity of MLN KO mice, it is interesting to speculate that pharmacologic approaches to disrupt the association of MLN with SERCA might have similar salutary effects. Modulation of SERCA activity in skeletal muscle has also been implicated in the control of systemic energy homeostasis (Bal et al., 2012), raising the interesting possibility that MLN may exert additional metabolic functions. Considering that SERCA is also important in Ca^{2+} regulation in non-muscle cell types in which MLN, PLN and SLN are not expressed, it is interesting to speculate that additional SERCA-modulating micropeptides may be concealed within putative lncRNAs expressed in other tissues. Finally, the discovery of MLN as a previously unrecognized regulator of muscle function suggests that the microproteome, which is largely unexplored, represents a reservoir for future biological insights.

Experimental Procedures

TALEN-mediated Homologous Recombination in Mice

A unique TALEN pair specific for the MLN locus was designed using the ZiFiT Targeter Program (http://zifit.partners.org/ZiFiT/Introduction.aspx) and constructed using the REAL assembly kit (Addgene) (Reyon et al., 2012). A donor vector containing the tdTomato reporter and triple polyadenylation sequences was constructed by incorporating short 5' and 3' homology arms specific to the MLN locus. TALEN mRNAs were in vitro transcribed using the mMessage mMachine T7 Ultra kit (Life Technologies), diluted to 25 ng μl^{-1}, and co-injected with 3 ng μl^{-1} of the circular DNA donor plasmid into the nucleus and cytoplasm of one-cell stage embryos (B6C3F1) and transferred into pseudopregnant female ICR mice.

Study Approval

All experimental procedures involving animals in this study were reviewed and approved by the University of Texas Southwestern Medical Center's Institutional Animal Care and Use Committee.

Radioisotopic In Situ Hybridization

In situ hybridizations were performed as previously described (Shelton et al., 2000). See Extended Experimental Procedures for a more detailed protocol. The primer sequences used to clone MLN, PLN and SLN cDNA templates are listed in Table S2.

CRISPR/Cas9-mediated Homologous Recombination in C2C12 Myoblasts

A single-guide RNA (sgRNA) specific to the C-terminal coding sequence of the mouse MLN locus was cloned into the sgRNA/Cas9 expression vector px330 (MLN-FLAG-px330). The donor vector was constructed with a single FLAG epitope tag in-frame with the MLN coding sequence flanked by ~500 base pair homology arms specific to the MLN

locus. MLN-FLAG knock-in clones were generated by transient co-transfection and expanded from single cell clones. Detection of endogenous MLN-FLAG peptide was performed by immunoblotting with a rabbit anti-FLAG antibody (Sigma) on protein lysates immunoprecipitated with mouse anti-FLAG agarose beads (Sigma).

Treadmill Running

In blinded studies, male MLN KO and WT littermate mice were subjected to forced exercise on a treadmill (Exer-6M, Columbus Instruments, 10% incline) at 8-weeks of age using a regimen previously described (van Rooij et al., 2009). See Extended Experimental Procedures for a more detailed protocol.

Intracellular Ca^{2+} Imaging

Cytosolic Ca^{2+} levels were measured as described previously (Liou et al., 2005) with the exception that retroviral transduced C2C12 cells or primary myoblasts were plated on Ibidi μ-35mm tissue-culture dishes and cultured for 24 hours in low Ca^{2+} (0.1 mM Ca^{2+}) prior to imaging to increase sensitivity to changes in SR Ca^{2+} levels (Brandman et al., 2007). SR Ca^{2+} levels were directly measured using T1ER as previously described (Abell et al., 2011; Tsai et al., 2014). See Extended Experimental Procedures for a more detailed protocol.

Oxalate-Supported Ca^{2+} Uptake Measurements in HEK293 Lysates

Oxalate supported Ca^{2+}-dependent Ca^{2+}-ATPase activity in homogenates was measured by a modification of the Millipore filtration technique as described in detail (Holemans et al., 2014; Luo et al., 1994). HEK293 cells were co-transfected with equal amounts of an expression plasmid encoding mouse SERCA1 and an expression plasmid encoding MLN, PLN or SLN. See Extended Experimental Procedures for a more detailed protocol.

Co-immunoprecipitations and Western Blot Analysis

Co-immunoprecipitations (CoIPs) were performed as previously described (Anderson et al., 2009). Tris-tricine-SDS PAGE was carried out using 16.5% Tris-tricine gels (BioRad) and Tris-tricine-SDS running buffer (BioRad). See Extended Experimental Procedures for a more detailed protocol.

Real-time PCR

Total RNA was prepared from whole muscles using Trizol (Invitrogen) and treated with DNase prior to reverse transcription by Superscript III (Invitrogen). Real-time RT-PCR was performed using TaqMan probes (ABI) or SYBR green using primers in Table S2. Taqman probes: Mck (Mm00432556_m1), Mef2c (Mm01340842_m1), SLN (Mm00481536_m1), PLN (Mm00452263_m1), SERCA2 (Mm01201434_m1). Primers for SYBR green reactions are listed in Table S2.

Electrophoretic Shift Assays

Electrophoretic shift assays (EMSA) were performed as previously described (Anderson et al., 2012) using recombinant myc-tagged proteins expressed in COS7 cells and double-stranded EMSA probes created by annealing complementary oligonucleotides. Probe

sequences are listed in Table S2. Supershifts were performed by adding 1 μg of mouse anti-Myc antibody (Invitrogen). See Extended Experimental Procedures for a more detailed protocol.

Luciferase Assays

Luciferase assays were performed as previously described (Anderson et al., 2009). Luciferase activity was measured using a FluoStar OPTIMA microplate reader (BMG Labtech) and normalized to beta-galactosidase activity using the FluoReporter LacZ/ Galactosidase Quantitation Kit (Invitrogen). See Extended Experimental Procedures for a more detailed protocol.

Subcellular Fractionation

C2C12 myoblasts infected with a retrovirus encoding the HA-MLN fusion protein (pBabeX-HA-MLN) were fractionated as previously described (Millay et al., 2013). See Extended Experimental Procedures for a more detailed protocol.

Northern and Southern Blot Analysis

Northern blots were performed using a commercially prepared adult mouse multi-tissue RNA blot (MN-MT-1, Zyagen) hybridized with a radiolabeled DNA probe specific to the full-length MLN transcript. Radiolabeled DNA probes for Northern and Southern blots were generated using a RadPrime kit (Invitrogen) (Table S2).

Histology and Immunohistochemistry

Skeletal muscle tissues were dissected and fixed overnight in 4% formaldehyde in PBS prior to paraffin embedding and sectioning using routine procedures. Immunohistochemistry was performed on deparaffinized sections using a HistoMouse-Plus kit (Invitrogen) using primary antibodies specific to fast (MY32, Sigma) and slow (NOQ7.54, Sigma) myosins. Wheat germ agglutinin (WGA) staining was performed using Alexa Fluor 555–conjugated WGA (Invitrogen) as described previously (Liu et al., 2011).

Analysis of RNA-seq Expression Data

Raw data for C2C12 cells and triceps brachii muscle were downloaded from the Short Read Archive (SRP002119 and SRP008123, respectively). Reads were mapped to the UCSC mm9 genome annotation using TopHat and alignments were processed to bigWig coverage maps and viewed using the UCSC genome browser.

Circular Dichroism Spectroscopy

Circular Dichroism (CD) spectroscopy measurements were done using a JASCO J-815 spectrometer on in vitro synthesized full-length MLN (Peptide 2.0 Inc.). The secondary structure elements were calculated using Yang's fit. The RMS deviation for the observed and calculated CD spectra values was 3%. See Extended Experimental Procedures for a more detailed protocol.

Structural Modeling and Automated Protein Docking

The helical domains of MLN, PLN, SLN and SCL were created ab initio using I-TASSER (Zhang, 2008). Automated protein docking of the MLN model with the crystal structure of SERCA1 (4H1W) was performed using ClusPro 2.0 (Comeau et al., 2004).

Adult Muscle Electroporation and Imaging

Flexor digitorum brevis (FDB) muscles of 12-week old male mice were electroporated as previously described (Nelson et al., 2013) with expression vectors encoding N-terminal GFP fusions to MLN, PLN or SLN. Unfixed FDB muscles were examined directly using two-photon laser scanning microscopy (Zeiss; LSM 780) with reverse second harmonic generation to visualize the A bands as an internal reference. See Extended Experimental Procedures for a more detailed protocol.

Supplementary Material

Refer to Web version on PubMed Central for supplementary material.

Acknowledgements

We thank Dr. Tobias Meyer at Stanford University Medical Center for generously providing the pcDNA-T1ER vector and Dr. David H. MacLennan at the University of Toronto for generously providing the Serca1 (A52) antibody. This work was supported by grants from the NIH (HL-077439, HL-111665, HL-093039, DK-099653 and U01-HL-100401), the Leducq Foundation and the Robert A. Welch Foundation (grant 1-0025 to E.N.O. and grant I-1789 to J.L.). D.M.A. was supported by an American Heart Association postdoctoral fellowship (13POST14570050). K.M.A. was supported by an American Heart Association pre-doctoral fellowship (14PRE19830031). B.R.N. was supported by an NIH Training grant (1F30AR067094-01), P.K. was supported by a postdoctoral grant from Sigrid Juselius Foundation.

References

Abell E, Ahrends R, Bandara S, Park BO, Teruel MN. Parallel adaptive feedback enhances reliability of the Ca2+ signaling system. Proc Natl Acad Sci U S A. 2011; 108:14485–14490. [PubMed: 21844332]

Allen DG, Gervasio OL, Yeung EW, Whitehead NP. Calcium and the damage pathways in muscular dystrophy. Can J Physiol Pharmacol. 2010; 88:83–91. [PubMed: 20237582]

Anderson DM, Beres BJ, Wilson-Rawls J, Rawls A. The homeobox gene Mohawk represses transcription by recruiting the sin3A/HDAC co-repressor complex. Dev Dyn. 2009; 238:572–580. [PubMed: 19235719]

Anderson DM, George R, Noyes MB, Rowton M, Liu W, Jiang R, Wolfe SA, Wilson-Rawls J, Rawls A. Characterization of the DNA-binding properties of the Mohawk homeobox transcription factor. J Biol Chem. 2012; 287:35351–35359. [PubMed: 22923612]

Andrews SJ, Rothnagel JA. Emerging evidence for functional peptides encoded by short open reading frames. Nat Rev Genet. 2014; 15:193–204. [PubMed: 24514441]

Anger M, Samuel JL, Marotte F, Wuytack F, Rappaport L, Lompre AM. In situ mRNA distribution of sarco(endo)plasmic reticulum Ca(2+)-ATPase isoforms during ontogeny in the rat. J Mol Cell Cardiol. 1994; 26:539–550. [PubMed: 8072009]

Bal NC, Maurya SK, Sopariwala DH, Sahoo SK, Gupta SC, Shaikh SA, Pant M, Rowland LA, Bombardier E, Goonasekera SA, et al. Sarcolipin is a newly identified regulator of muscle-based thermogenesis in mammals. Nat Med. 2012; 18:1575–1579. [PubMed: 22961106]

Bassel-Duby R, Olson EN. Signaling pathways in skeletal muscle remodeling. Annu Rev Biochem. 2006; 75:19–37. [PubMed: 16756483]

Bazzini AA, Johnstone TG, Christiano R, Mackowiak SD, Obermayer B, Fleming ES, Vejnar CE, Lee MT, Rajewsky N, Walther TC, et al. Identification of small ORFs in vertebrates using ribosome footprinting and evolutionary conservation. EMBO J. 2014

Berchtold MW, Brinkmeier H, Muntener M. Calcium ion in skeletal muscle: its crucial role for muscle function, plasticity, and disease. Physiol Rev. 2000; 80:1215–1265. [PubMed: 10893434]

Bernstein BE, Birney E, Dunham I, Green ED, Gunter C, Snyder M. An integrated encyclopedia of DNA elements in the human genome. Nature. 2012; 489:57–74. [PubMed: 22955616]

Berridge MJ, Bootman MD, Roderick HL. Calcium signalling: dynamics, homeostasis and remodelling. Nat Rev Mol Cell Biol. 2003; 4:517–529. [PubMed: 12838335]

Brandman O, Liou J, Park WS, Meyer T. STIM2 is a feedback regulator that stabilizes basal cytosolic and endoplasmic reticulum Ca2+ levels. Cell. 2007; 131:1327–1339. [PubMed: 18160041]

Briggs FN, Lee KF, Wechsler AW, Jones LR. Phospholamban expressed in slow-twitch and chronically stimulated fast-twitch muscles minimally affects calcium affinity of sarcoplasmic reticulum Ca(2+)-ATPase. J Biol Chem. 1992; 267:26056–26061. [PubMed: 1464616]

Chu G, Ferguson DG, Edes I, Kiss E, Sato Y, Kranias EG. Phospholamban ablation and compensatory responses in the mammalian heart. Ann N Y Acad Sci. 1998; 853:49–62. [PubMed: 10603936]

Comeau SR, Gatchell DW, Vajda S, Camacho CJ. ClusPro: an automated docking and discrimination method for the prediction of protein complexes. Bioinformatics. 2004; 20:45–50. [PubMed: 14693807]

Dorn GW 2nd, Molkentin JD. Manipulating cardiac contractility in heart failure: data from mice and men. Circulation. 2004; 109:150–158. [PubMed: 14734503]

Fajardo VA, Bombardier E, Vigna C, Devji T, Bloemberg D, Gamu D, Gramolini AO, Quadrilatero J, Tupling AR. Co-expression of SERCA isoforms, phospholamban and sarcolipin in human skeletal muscle fibers. PLoS One. 2013; 8:e84304. [PubMed: 24358354]

Fong AP, Yao Z, Zhong JW, Cao Y, Ruzzo WL, Gentleman RC, Tapscott SJ. Genetic and epigenetic determinants of neurogenesis and myogenesis. Dev Cell. 2012; 22:721–735. [PubMed: 22445365]

Goonasekera SA, Lam CK, Millay DP, Sargent MA, Hajjar RJ, Kranias EG, Molkentin JD. Mitigation of muscular dystrophy in mice by SERCA overexpression in skeletal muscle. J Clin Invest. 2011; 121:1044–1052. [PubMed: 21285509]

Holemans T, Vandecaetsbeek I, Wuytack F, Vangheluwe P. Measuring Ca2+-dependent Ca2+-uptake activity in the mouse heart. Cold Spring Harb Protoc. 2014; 2014:876–886.

Kirchberber MA, Tada M, Katz AM. Phospholamban: a regulatory protein of the cardiac sarcoplasmic reticulum. Recent Adv Stud Cardiac Struct Metab. 1975; 5:103–115. [PubMed: 127351]

Kranias EG, Hajjar RJ. Modulation of cardiac contractility by the phospholamban/SERCA2a regulatome. Circ Res. 2012; 110:1646–1660. [PubMed: 22679139]

Liu N, Bezprozvannaya S, Shelton JM, Frisard MI, Hulver MW, McMillan RP, Wu Y, Voelker KA, Grange RW, Richardson JA, et al. Mice lacking microRNA 133a develop dynamin 2-dependent centronuclear myopathy. J Clin Invest. 2011; 121:3258–3268. [PubMed: 21737882]

Lu BD, Allen DL, Leinwand LA, Lyons GE. Spatial and temporal changes in myosin heavy chain gene expression in skeletal muscle development. Dev Biol. 1999; 216:312–326. [PubMed: 10588881]

Luo W, Grupp IL, Harrer J, Ponniah S, Grupp G, Duffy JJ, Doetschman T, Kranias EG. Targeted ablation of the phospholamban gene is associated with markedly enhanced myocardial contractility and loss of beta-agonist stimulation. Circ Res. 1994; 75:401–409. [PubMed: 8062415]

MacLennan DH, Asahi M, Tupling AR. The regulation of SERCA-type pumps by phospholamban and sarcolipin. Ann N Y Acad Sci. 2003; 986:472–480. [PubMed: 12763867]

MacLennan DH, Kranias EG. Phospholamban: a crucial regulator of cardiac contractility. Nat Rev Mol Cell Biol. 2003; 4:566–577. [PubMed: 12838339]

Magny EG, Pueyo JI, Pearl FM, Cespedes MA, Niven JE, Bishop SA, Couso JP. Conserved regulation of cardiac calcium uptake by peptides encoded in small open reading frames. Science. 2013; 341:1116–1120. [PubMed: 23970561]

Mattiazzi A, Mundina-Weilenmann C, Vittone L, Said M, Kranias EG. The importance of the Thr17 residue of phospholamban as a phosphorylation site under physiological and pathological conditions. Braz J Med Biol Res. 2006; 39:563–572. [PubMed: 16648892]

Millay DP, O'Rourke JR, Sutherland LB, Bezprozvannaya S, Shelton JM, Bassel-Duby R, Olson EN. Myomaker is a membrane activator of myoblast fusion and muscle formation. Nature. 2013; 499:301–305. [PubMed: 23868259]

Millay DP, Sargent MA, Osinska H, Baines CP, Barton ER, Vuagniaux G, Sweeney HL, Robbins J, Molkentin JD. Genetic and pharmacologic inhibition of mitochondrial-dependent necrosis attenuates muscular dystrophy. Nat Med. 2008; 14:442–447. [PubMed: 18345011]

Minamisawa S, Wang Y, Chen J, Ishikawa Y, Chien KR, Matsuoka R. Atrial chamber-specific expression of sarcolipin is regulated during development and hypertrophic remodeling. J Biol Chem. 2003; 278:9570–9575. [PubMed: 12645548]

Nelson BR, Wu F, Liu Y, Anderson DM, McAnally J, Lin W, Cannon SC, Bassel-Duby R, Olson EN. Skeletal muscle-specific T-tubule protein STAC3 mediates voltage-induced Ca2+ release and contractility. Proc Natl Acad Sci U S A. 2013; 110:11881–11886. [PubMed: 23818578]

Odermatt A, Taschner PE, Khanna VK, Busch HF, Karpati G, Jablecki CK, Breuning MH, MacLennan DH. Mutations in the gene-encoding SERCA1, the fast-twitch skeletal muscle sarcoplasmic reticulum Ca2+ ATPase, are associated with Brody disease. Nat Genet. 1996; 14:191–194. [PubMed: 8841193]

Odermatt A, Taschner PE, Scherer SW, Beatty B, Khanna VK, Cornblath DR, Chaudhry V, Yee WC, Schrank B, Karpati G, et al. Characterization of the gene encoding human sarcolipin (SLN), a proteolipid associated with SERCA1: absence of structural mutations in five patients with Brody disease. Genomics. 1997; 45:541–553. [PubMed: 9367679]

Pan Y, Zvaritch E, Tupling AR, Rice WJ, de Leon S, Rudnicki M, McKerlie C, Banwell BL, MacLennan DH. Targeted disruption of the ATP2A1 gene encoding the sarco(endo)plasmic reticulum Ca2+ ATPase isoform 1 (SERCA1) impairs diaphragm function and is lethal in neonatal mice. J Biol Chem. 2003; 278:13367–13375. [PubMed: 12556521]

Periasamy M, Kalyanasundaram A. SERCA pump isoforms: their role in calcium transport and disease. Muscle Nerve. 2007; 35:430–442. [PubMed: 17286271]

Reyon D, Khayter C, Regan MR, Joung JK, Sander JD. Engineering designer transcription activator-like effector nucleases (TALENs) by REAL or REAL-Fast assembly. Curr Protoc Mol Biol Chapter. 2012; 12 Unit 12 15.

Rossi AE, Dirksen RT. Sarcoplasmic reticulum: the dynamic calcium governor of muscle. Muscle Nerve. 2006; 33:715–731. [PubMed: 16477617]

Schmitt JP, Kamisago M, Asahi M, Li GH, Ahmad F, Mende U, Kranias EG, MacLennan DH, Seidman JG, Seidman CE. Dilated cardiomyopathy and heart failure caused by a mutation in phospholamban. Science. 2003; 299:1410–1413. [PubMed: 12610310]

Shelton JM, Lee MH, Richardson JA, Patel SB. Microsomal triglyceride transfer protein expression during mouse development. J Lipid Res. 2000; 41:532–537. [PubMed: 10744773]

Slack JP, Grupp IL, Luo W, Kranias EG. Phospholamban ablation enhances relaxation in the murine soleus. Am J Physiol. 1997; 273:C1–C6. [PubMed: 9252436]

Tada M, Toyofuku T. Molecular regulation of phospholamban function and expression. Trends Cardiovasc Med. 1998; 8:330–340. [PubMed: 14987547]

Toyoshima C, Asahi M, Sugita Y, Khanna R, Tsuda T, MacLennan DH. Modeling of the inhibitory interaction of phospholamban with the Ca2+ ATPase. Proc Natl Acad Sci U S A. 2003; 100:467–472. [PubMed: 12525698]

Toyoshima C, Iwasawa S, Ogawa H, Hirata A, Tsueda J, Inesi G. Crystal structures of the calcium pump and sarcolipin in the Mg2+-bound E1 state. Nature. 2013; 495:260–264. [PubMed: 23455422]

Tsai FC, Seki A, Yang HW, Hayer A, Carrasco S, Malmersjo S, Meyer T. A polarized Ca2+, diacylglycerol and STIM1 signalling system regulates directed cell migration. Nat Cell Biol. 2014; 16:133–144. [PubMed: 24463606]

Tupling AR, Bombardier E, Gupta SC, Hussain D, Vigna C, Bloemberg D, Quadrilatero J, Trivieri MG, Babu GJ, Backx PH, et al. Enhanced Ca2+ transport and muscle relaxation in skeletal muscle from sarcolipin-null mice. Am J Physiol Cell Physiol. 2011; 301:C841–C849. [PubMed: 21697544]

van Rooij E, Quiat D, Johnson BA, Sutherland LB, Qi X, Richardson JA, Kelm RJ Jr, Olson EN. A family of microRNAs encoded by myosin genes governs myosin expression and muscle performance. Dev Cell. 2009; 17:662–673. [PubMed: 19922871]

Vangheluwe P, Schuermans M, Zador E, Waelkens E, Raeymaekers L, Wuytack F. Sarcolipin and phospholamban mRNA and protein expression in cardiac and skeletal muscle of different species. Biochem J. 2005; 389:151–159. [PubMed: 15801907]

Wawrzynow A, Theibert JL, Murphy C, Jona I, Martonosi A, Collins JH. Sarcolipin, the “proteolipid” of skeletal muscle sarcoplasmic reticulum, is a unique, amphipathic, 31-residue peptide. Arch Biochem Biophys. 1992; 298:620–623. [PubMed: 1416990]

Wegener AD, Simmerman HK, Lindemann JP, Jones LR. Phospholamban phosphorylation in intact ventricles. Phosphorylation of serine 16 and threonine 17 in response to beta-adrenergic stimulation. J Biol Chem. 1989; 264:11468–11474. [PubMed: 2544595]

Winther AM, Bublitz M, Karlsen JL, Moller JV, Hansen JB, Nissen P, Buch-Pedersen MJ. The sarcolipin-bound calcium pump stabilizes calcium sites exposed to the cytoplasm. Nature. 2013; 495:265–269. [PubMed: 23455424]

Zhang Y. I-TASSER server for protein 3D structure prediction. BMC Bioinformatics. 2008; 9:40. [PubMed: 18215316]

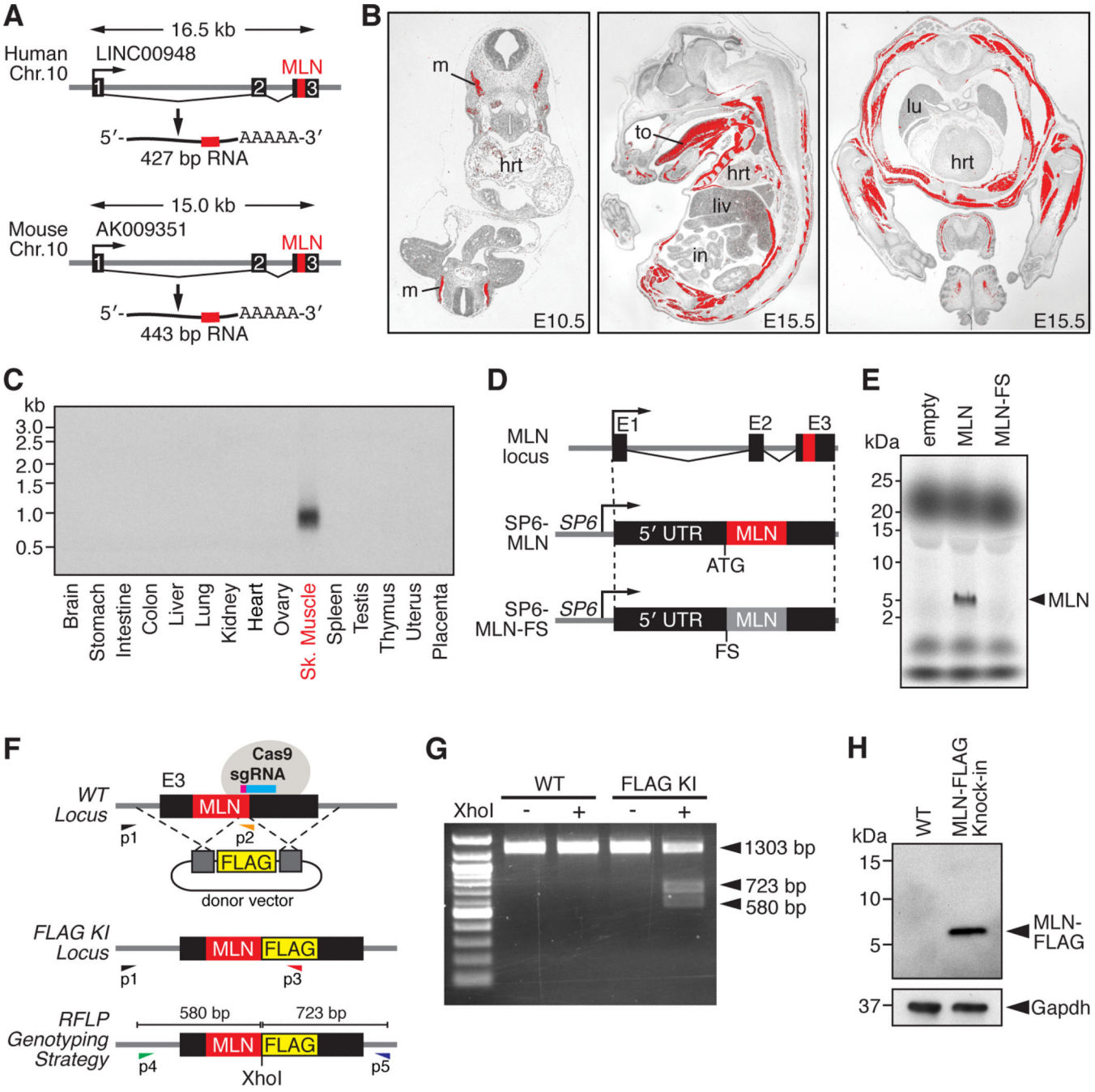

Figure 1. Discovery of a Skeletal Muscle-specific Micropeptide

(A) A short ORF encoding a conserved micropeptide, that we named myoregulin (MLN), is contained within exon 3 of an annotated lncRNA in human and mouse genomes. The position of the MLN ORF is indicated in red.

(B) In situ hybridization showing skeletal muscle-specific expression of MLN at the indicated embryonic time-points. (hrt, heart; in, intestine; liv, liver; lu, lung; m, myotome; to, tongue)

(C) Northern blot of RNA isolated from adult mouse tissues using a probe specific to the full-length MLN transcript shows skeletal muscle-specific expression.
(D) Diagram of the constructs used for in vitro translation of the MLN micropeptide. The full-length MLN RNA transcript was subcloned into the CS2 vector containing the SP6 phage RNA polymerase promoter (SP6-MLN). A frameshift mutation was introduced immediately after the endogenous ATG to disrupt the MLN ORF (SP6-MLN-FS).
(E) Coupled in vitro transcription and translation reactions of the SP6-MLN vector using radiolabeled ^{35}S-methionine produced a ∼5 kDa micropeptide, visualized by Tricine SDS-PAGE. The frame-shift mutation in the MLN ORF (SP6-MLN-FS) abolished any detectable expression.
(F) Targeting strategy using CRISPR/Cas9-mediated homologous recombination to knock-in a FLAG epitope tag into the MLN locus in C2C12 cells. PCR-based genotyping using primers (P1-P3) or RFLP analysis of PCR products generated using primers (P4 and P5) were used to verify correct targeting.
(G) RFLP analysis of WT C2C12 and heterozygous C2C12 myoblasts for the MLN-FLAG knock-in allele.
(H) Western blot analysis showing endogenous expression of the MLN-FLAG fusion peptide in differentiated C2C12 myotubes, detected with an anti-FLAG antibody.
See also Figure S1.

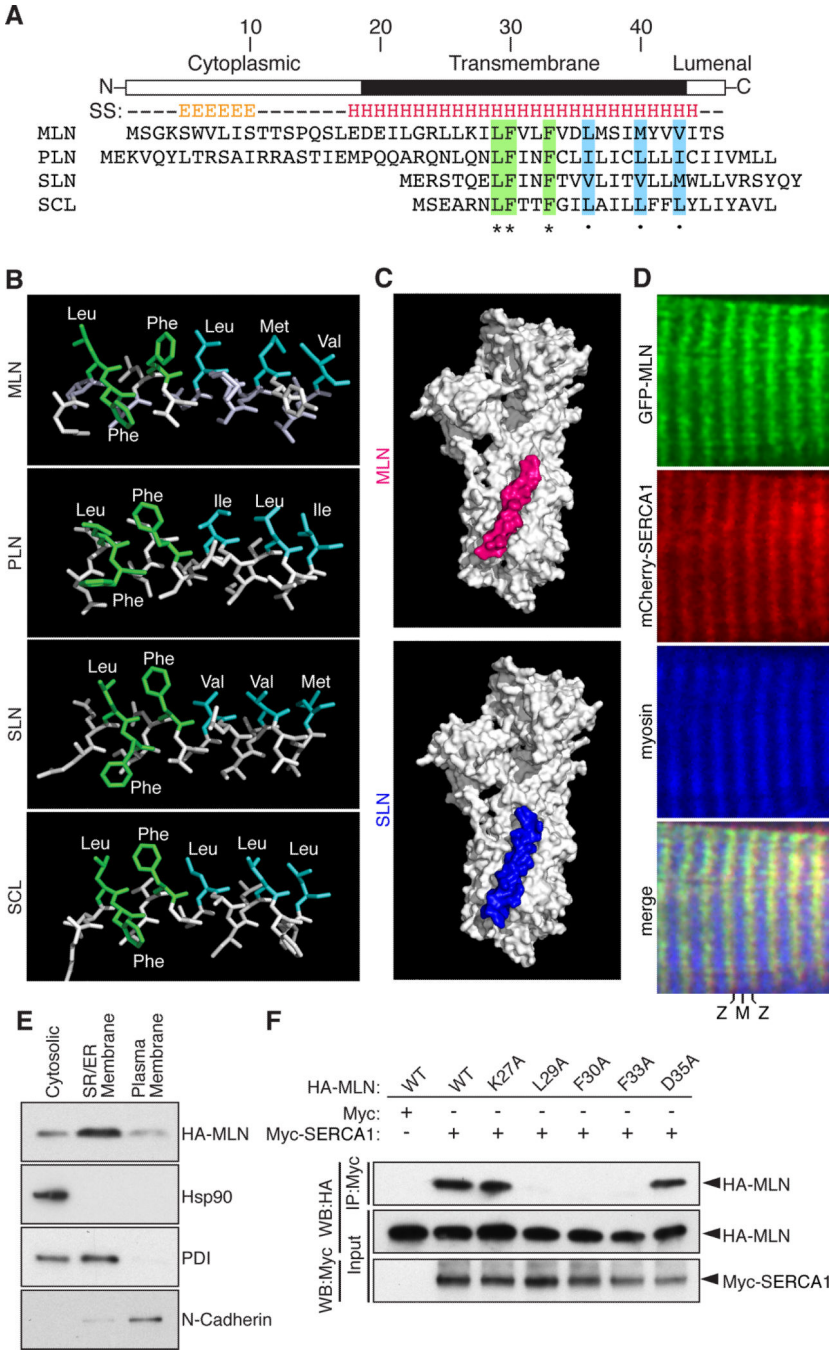

Figure 2. MLN Forms a Transmembrane Alpha Helix that Interacts with SERCA

(A) The secondary structure (SS) of MLN is predicted to contain an N-terminal beta sheet and C-terminal transmembrane alpha helix (E, beta sheet; H, alpha helix). Alignment of mouse MLN, PLN, SLN and the invertebrate ortholog SCL identified identical (green) and similar (blue) residues conserved in all four micropeptides.

(B) The structure of the transmembrane helices of MLN, SLN, PLN and SCL was modeled using I-TASSER and showed a common spatial orientation of conserved residues.

(C) Automated protein docking using ClusPro predicted that MLN occupies the same groove in SERCA1 that is recognized by SLN.
(D) Expression of GFP-MLN and mCherry-SERCA1 fusion proteins in mature skeletal muscle fibers, showing co-localization in the SR, imaged using two-photon laser scanning confocal microscopy. (M, M-line; Z, Z-line)
(E) Retroviral expression of an N-terminal HA-tagged MLN fusion peptide (HA-MLN) in C2C12 myoblasts was enriched in the subcellular fraction containing SR/ER membrane proteins. Enrichment for cytosolic, SR/ER membrane and plasma membrane proteins was verified by Western blot analysis for Hsp90, PDI and N-Cadherin, respectively.
(F) Co-immunoprecipitation (CoIP) experiments with HA-tagged MLN alanine mutants and a Myc-tagged SERCA1 construct transfected into COS7 cells identified residues important for interaction of MLN with SERCA1. Interaction of MLN with SERCA1 was abolished by mutation of residues shared with PLN, SLN and SCL (L29A, F30A and F33A) but not by the charged residues K27A or D35A. Western blot performed with anti-HA (WB-HA) or anti-Myc (WB-Myc). See also Figure S2.

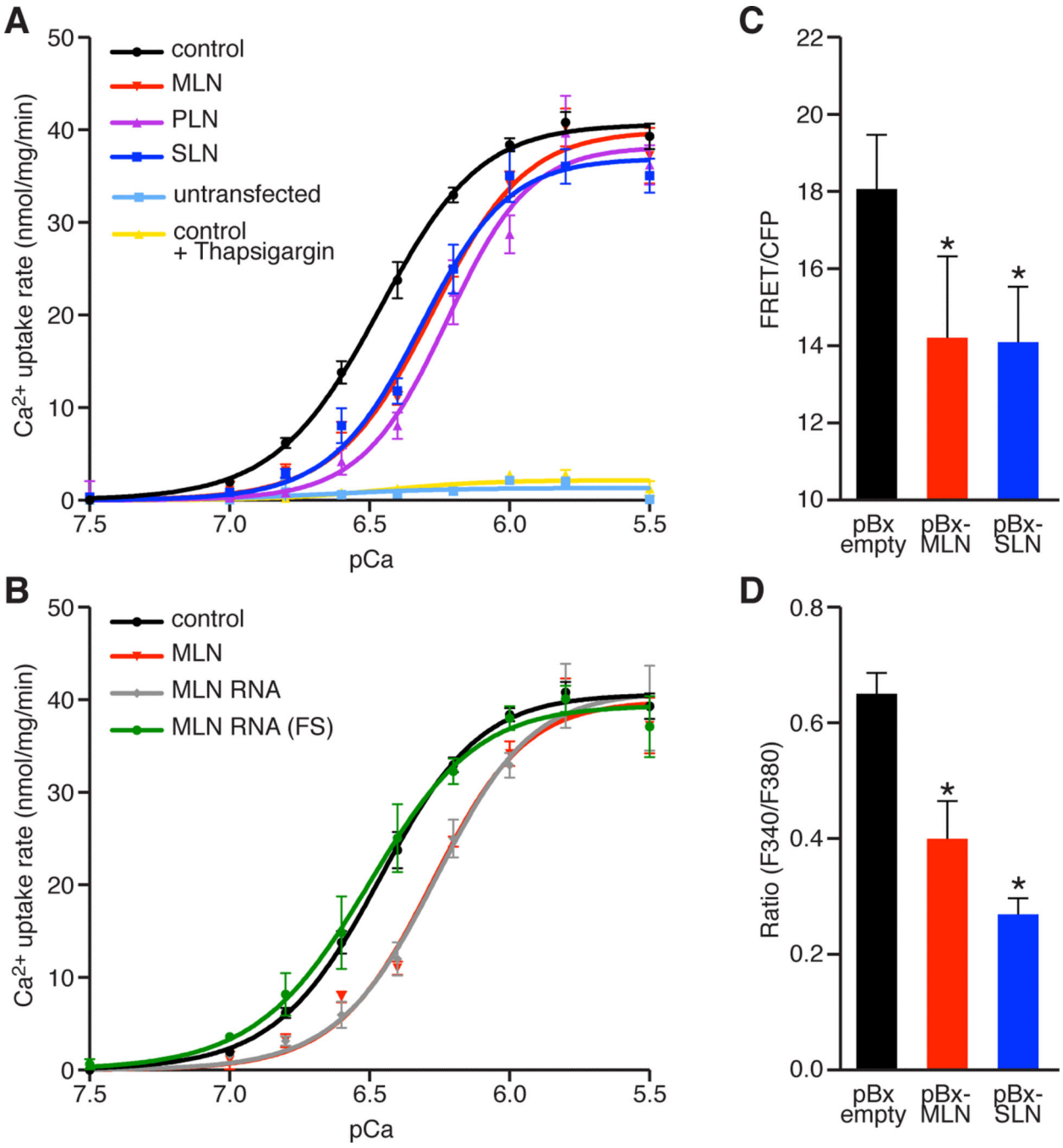

Figure 3. MLN Regulates SR Ca^{2+} Levels by Inhibiting SERCA Pump Activity

(A and B) The Ca^{2+}-dependence of the relative rate of Ca^{2+} uptake is shown for homogenates from HEK 293 cells co-transfected with SERCA1 and the indicated constructs. Co-transfection with MLN, PLN or SLN resulted in a similar decrease in Ca^{2+} uptake, corresponding to a decreased affinity of SERCA for Ca^{2+}, relative to empty vector (Control). For comparison, untransfected cells and SERCA1 expressing cells treated with the SERCA inhibitor thapsigargin (100nM) are shown. The activity of the full-length RNA

transcript encoding the MLN ORF (MLN RNA) is abolished by a frameshift mutation in the MLN ORF (MLN-RNA FS).

(C) Retroviral co-transduction of C2C12 myoblasts with the FRET-based Ca^{2+} sensor T1ER with MLN or SLN was used to directly measure the relative levels of SR Ca^{2+}. Both MLN and SLN significantly decreased SR Ca^{2+} levels relative to an empty retroviral vector.

(D) Retroviral over-expression of MLN or SLN in C2C12 myoblasts treated with 4-CMC and imaged with fura-2-AM showed decreased levels of SR Ca^{2+}, measured by peak Ca^{2+} release from the SR.

Data are presented as mean ± SEM. (* denotes $p < 0.05$ compared to pBx-empty).

See also Table S1.

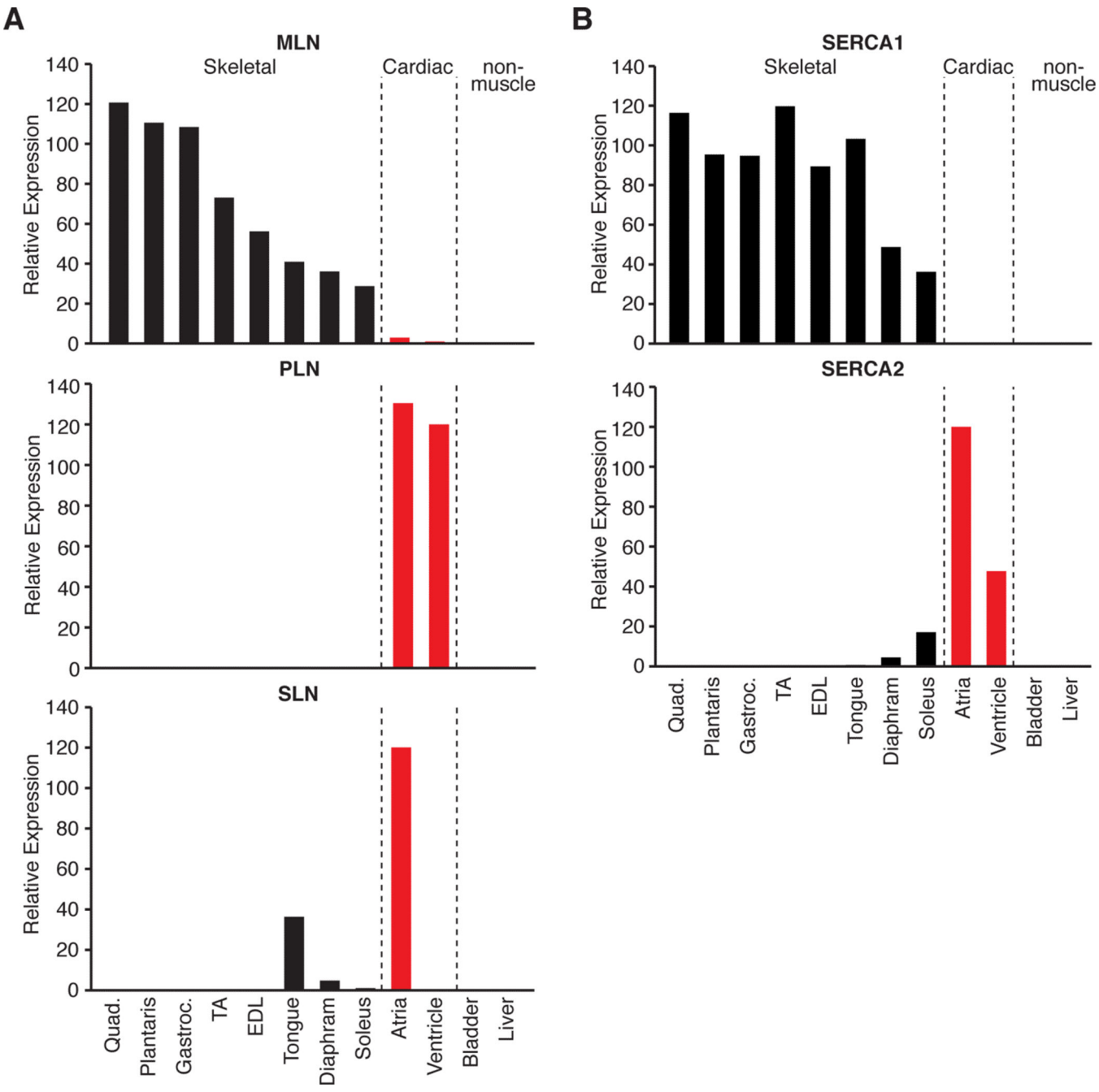

Figure 4. Developmental and Adult Expression of MLN, PLN and SLN in the Mouse

(A and B) Real-time PCR showing the relative expression of MLN, PLN, SLN and SERCA isoforms across multiple skeletal muscles, cardiac and non-muscle tissues isolated and pooled from three adult 8-week old C57Bl/6 male mice.

See also Figure S3.

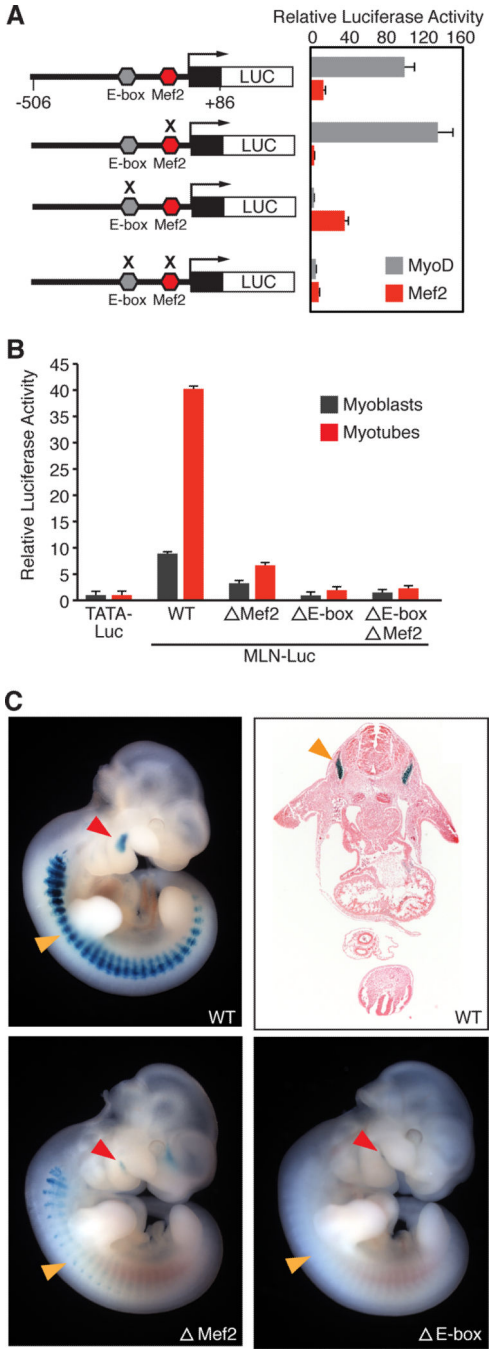

Figure 5. Regulation of MLN Transcription by MyoD and MEF2

(A) A fragment of the MLN promoter (−506 to +86, relative to the transcriptional start site) containing a highly conserved MyoD E-box (CACCTG) and MEF2 site (CTAATAACAG) was cloned in front of the luciferase reporter gene (MLN-Luc). The MLN-Luc reporter was robustly transactivated by the skeletal muscle transcription factors MyoD and MEF2 in COS7 cells (gray and red bars respectively). Mutation of the E-box (acCCgt) or Mef2 site (CTgggAACAG) (indicated by an X) abrogated transactivation by MyoD:E12 heterodimer

or Mef2c, respectively. All luciferase values were normalized to the transactivation of a basal luciferase reporter (TATA-Luc) with MyoD or Mef2, respectively.
(B) Transfection of the MLN-Luc reporter or mutant luciferase vectors into C2C12 myoblasts or myotubes showed they are essential for the transactivation of the MLN promoter.
(C) X-gal and H&E staining of E10.5 mouse embryos harboring either the MLN promoter-lacZ transgene (WT) or mutations in the MLN promoter (ΔMef2 or ΔE-box). The MLN-promoter showed expression in the myotomal compartment of the somites (orange arrow) and premyogenic cells in the mandibular arch (red arrow). Mutation of the MEF2 or E-box sequences in the MLN promoter-lacZ transgene abrogated or abolished muscle specific expression.
See also Figure S4.

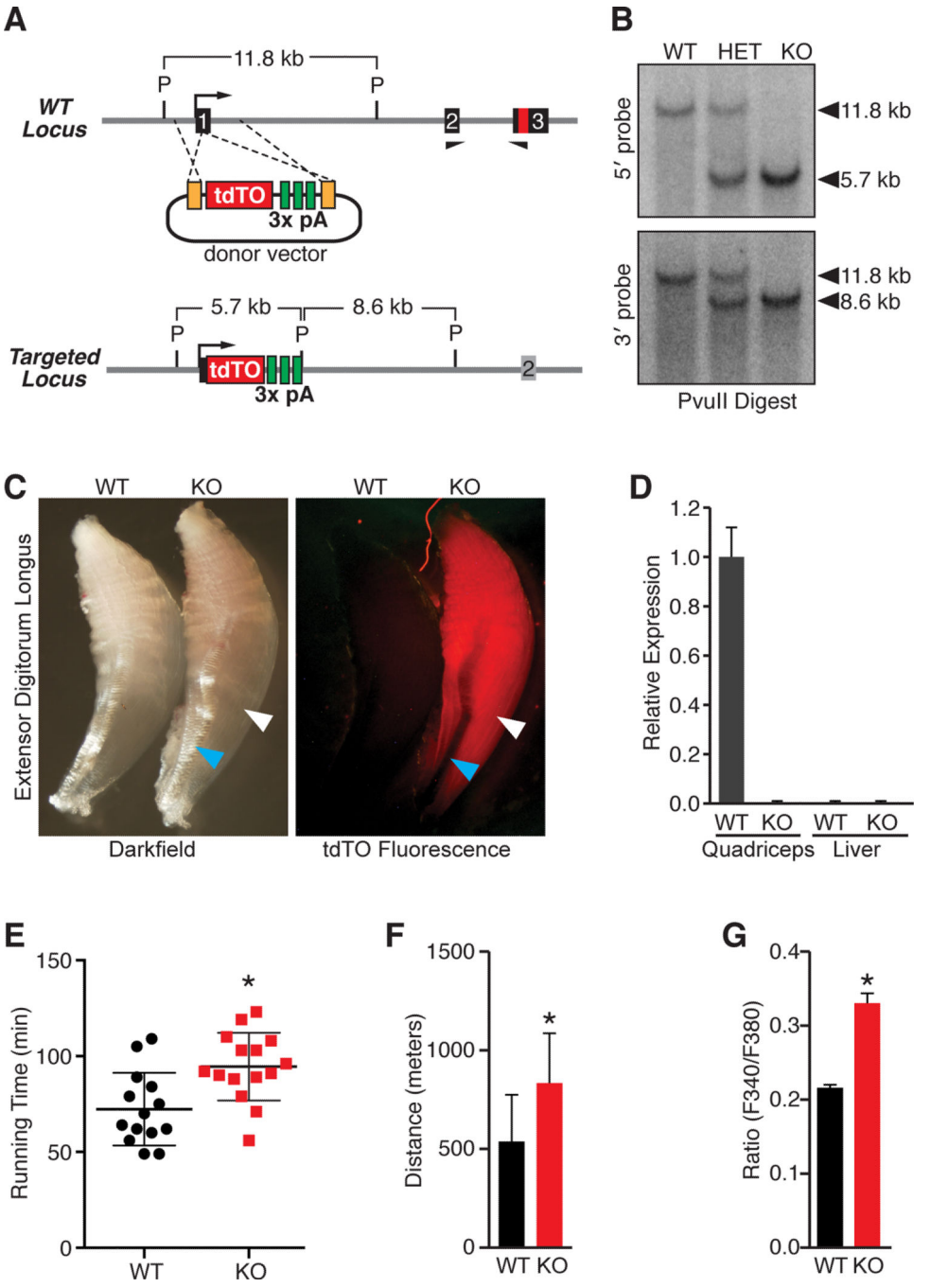

Figure 6. Generation and Characterization of MLN Knockout Mice

(A) TALEN-mediated homologous recombination was used to insert a tdTomato fluorescent reporter and triple polyadenylation cassette into exon 1 of the MLN locus to generate a null allele. A schematic of the donor vector and targeting strategy is shown. (P, PvuII)

(B) Southern blot analysis confirming correct targeting of the tdTO-triple polyadenylation cassette into exon 1 of the MLN locus using probes 5' and 3' to the TALEN cut site.

(C) tdTomato fluorescence was specific to skeletal muscle (white arrowhead) of MLN KO mice and not detected in other tissues, such as tendon (blue arrowhead).

(D) Real-time PCR using primers specific to exon 2 and 3 demonstrating absence of MLN transcripts in MLN KO muscle, as well as in liver.
(E) Muscle performance was measured using forced treadmill running to exhaustion. MLN KO (N=15) mice ran ∼31% longer than WT littermates (N=14).
(F) Comparison of distance run by MLN KO and WT mice in Figure 6E.
(G) Myoblasts isolated and cultured from MLN KO hindlimb muscles were imaged using Fura-2-AM and treated with the RyR agonist 4-CMC in the absence of extracellular Ca^{2+}, to indirectly measure SR Ca^{2+} levels. MLN KO myoblasts showed signigicantly increased SR Ca^{2+} levels, measured as peak Ca^{2+} release from the SR. Data are presented as mean ± SEM. (* denotes $p < 0.05$ compared to WT as in (E and F) and pBx-empty in (G)). See also Figure S5.

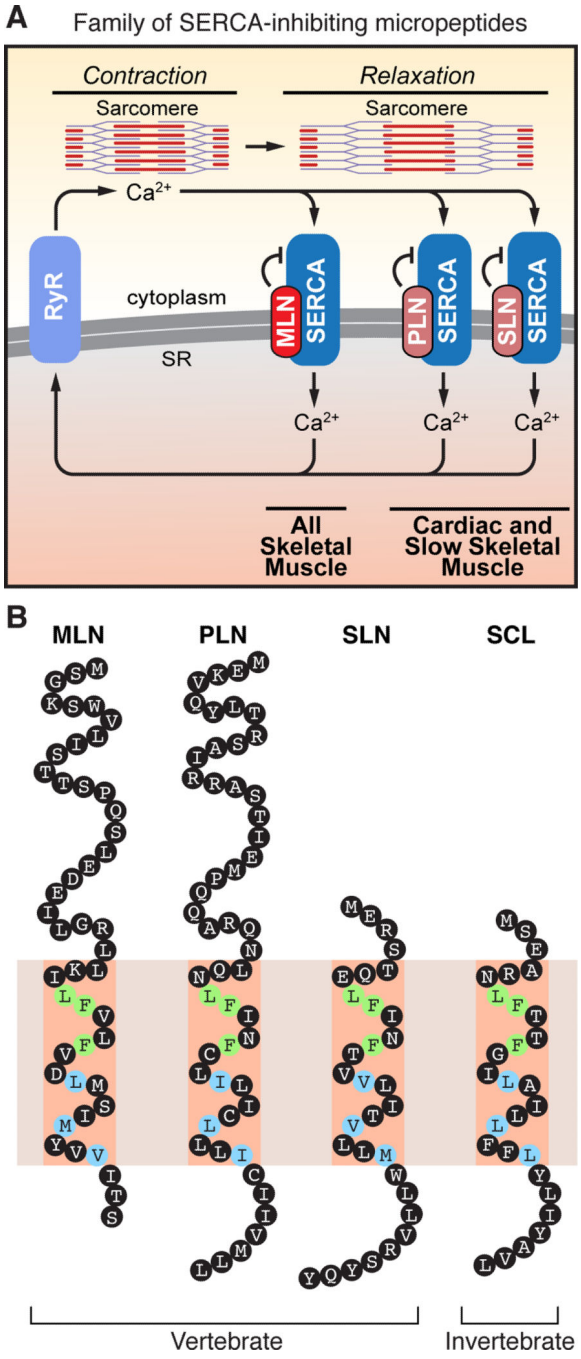

Figure 7. A Family of SERCA-inhibitory Micropeptides

(A) The Ca^{2+} pumps, RyR and SERCA, play a critical role in muscle contractility by controlling Ca^{2+} cycling between the cytosol and SR. MLN, PLN and SLN inhibit SERCA pump activity in different striated muscle types of vertebrates.

(B) Illustration of the family of SERCA-inhibitory micropeptides. The discovery of MLN reveals that vertebrates encode three SERCA-inhibitory peptides that share conserved residues within their transmembrane alpha helices. Green shading denotes identical residues

and blue denotes similar residues. MLN, myoregulin; PLN, phospholamban; SLN, sarcolipin; SCL, sarcolamban.